pendent (±0.01 ppm)[28] so this can be excluded as the dominate cause for the low-temperature deviations. Hence, simultaneous population of two states within this temperature range is consistent with the present data, but solid-state magnetic susceptibility measurements are required to prove this conclusively.

Conclusion

Heterobimetallic DPB complexes for all possible transition-metal combinations appear to be accessible with this straightforward, albeit lengthy, synthetic procedure. These developments may then lead to the preparation of porphyrin dimers with heteronuclear multiple bonds between 3d and 5d metals of the same triad, or more interestingly, between metals from different triads. In this study, we have chosen a trivial example of a heteronuclear metal–metal multiple bond, Os═Ru, to demonstrate that the cofacial bis(porphyrin) ligand can control the reaction stoichiometry and facilitates the formation of the intramolecular metal–metal bond. The stability of low oxidation states and the coordination chemistry necessary for the formation of the metal–metal bond (eq 6 and 8) are very similar for these two metals. This has made all the synthetic steps exactly analogous to those of the osmium and ruthenium complexes and allowed for two convergent steps. The syntheses for more interesting combintions, such as early–late transition metals (i.e., Mo═Ru), will probably not be as straightforward. The disparity between low oxidation state stabilities and the coordination chemistry of the two metalloporphyrins may still frustrate the synthesis. However, we nevertheless view this general synthetic procedure as an important step in the preparation of complexes with heteronuclear metal–metal multiple bonds.

We also anticipate benefits from these results in the area of electrocatalysis. The ability to prepare heterodinuclear DPB complexes with a 4d or 5d metal known to bind dinitrogen and another metal to activate it toward multielectron reduction should facilitate the survey of possible catalysts for this challenging catalytic reaction.

Acknowledgment. This work was supported by the National Science Foundation (Grant CHE83-18512). The NMR instrument was also funded by the National Science Foundation (Grant CHE81-09064). We thank Pat Bethel for LSI and FD mass spectral analyses of the new compounds at the Mass Spectroscopy Facility (A. L. Burlingame, Director) at the University of California, San Francisco, which is supported by the NIH Division of Research Resources, Grant RR01614, and Yunkyoung Ha for some assistance in the preparation of the latter compounds. This work is dedicated to J.M.G.'s father, James H. Garner.

---

[28] The maximum solubility of (Os)(Ru)DPB in benzene is approximately 3 mg/mL so the concentration range investigated was 0.2–0.7 mM.

ESR of Homo- and Heteroleptic Mono- and Dinuclear Tris(α-diimine)ruthenium Radical Complexes

Wolfgang Kaim,* Sylvia Ernst,[1] and Volker Kasack

Contribution from the Institut für Anorganische Chemie, Universität Stuttgart, Pfaffenwaldring 55, D-7000 Stuttgart 80, West Germany. *Received March 1, 1989*

Abstract: A comprehensive ESR study of 11 mononuclear and 5 dinuclear singly reduced tris(α-diimine)ruthenium(II) complexes of the general formulas $[(L)_3Ru]^{\bullet+}$, $[(L)(bpy)_2Ru]^{\bullet+}$, and $[(bpy)_2Ru(\mu\text{-}L)Ru(bpy)_2]^{\bullet3+}$ (bpy, 2,2′-bipyridine; L, other α-diimine) shows a variety of g factors and spectral resolution. All paramagnetic species are true anion-radical complexes with little g anisotropy and relatively small but characteristically positive differences g(ligand radical) − g(complex). The variations correlate with the calculated properties of the ligands and with spectroscopic and electrochemical data for the diamagnetic precursor complexes. In particular, the g shifts depend (i) on the extent of metal–ligand interaction and (ii) on the energy differences between the singly occupied and neighboring unoccupied or completely filled orbitals. Virtually complete localization of the unpaired electron on the better π-accepting ligand L has been established for the mono- and dinuclear heteroleptic systems, while fast spin exchange on the ESR time scale is evident from the ESR line width of all singly reduced homoleptic complexes.

The problem of (de)localization has been intensely debated in two areas of ruthenium ammine chemistry: One area has been the metal–metal interaction in the Creutz–Taube ion[2a] and related metal–metal mixed-valent species;[2] the other controversy surrounds the ligand–ligand mixed valency in reduced[3] or MLCT excited states[4] of tris(α-diimine)ruthenium complexes. Molecular ions such as $[Ru(bpy)_3]^{2+}$ are reversibly reduced[5,6] to anion-radical complexes (eq 1);[3a,b,7] the enormous attention devoted to this[4] and related complexes[5,8] stems from their use as photosensitizers, e.g., in water activation processes.[9]

---

[1] Present address: Beilstein-Institut fuer Organische Chemie, D-6000 Frankfurt/Main, West Germany.

[2] (a) Creutz, C.; Taube, H. *J. Am. Chem. Soc.* **1969**, *91*, 3988; **1973**, *95*, 1086. (b) Creutz, C. *Prog. Inorg. Chem.* **1983**, *30*, 1. (c) Richardson, D. E.; Taube, H. *Coord. Chem. Rev.* **1984**, *60*, 107. (d) Ernst, S.; Kasack, V.; Kaim, W. *Inorg. Chem.* **1988**, *27*, 1146.

[3] (a) Motten, A. G.; Hanck, K. W.; DeArmond, M. K. *Chem. Phys. Lett.* **1981**, *79*, 541. (b) Morris, D. E.; Hanck, K. W.; DeArmond, M. K. *J. Am. Chem. Soc.* **1983**, *105*, 3032. (c) *J. Electroanal. Chem.* **1983**, *149*, 115. (d) *Inorg. Chem.* **1985**, *24*, 977. (e) DeArmond, M. K.; Hanck, K. W.; Wertz, D. W. *Coord. Chem. Rev.* **1985**, *64*, 65. (f) Ohsawa, Y.; DeArmond, M. K.; Hanck, K. W.; Moreland, C. G. *J. Am. Chem. Soc.* **1985**, *107*, 5383. (g) Tait, C. T.; MacQueen, D. B.; Donohoe, R. J.; DeArmond, M. K.; Hanck, K. W.; Wertz, D. W. *J. Phys. Chem.* **1986**, *90*, 1766. (h) Gex, J. N.; DeArmond, M. K.; Hanck, K. W. *Ibid.* **1987**, *91*, 251. (i) Gex, J. N.; Cooper, J. B.; Hanck, K. W.; DeArmond, M. K. *Ibid.* **1987**, *91*, 4686. (j) Gex, J. N.; Brewer, W.; Bergmann, K.; Tait, C. D.; DeArmond, M. K.; Hanck, K. W.; Wertz, D. W. *Ibid.* **1987**, *91*, 4776. (k) Tait, C. D.; Vess, T. M.; DeArmond, M. K.; Hanck, K. W.; Wertz, D. W. *J. Chem. Soc., Dalton Trans.* **1987**, 2467. (l) Gex, J. N.; DeArmond, M. K.; Hanck, K. W. *Inorg. Chem.* **1987**, *26*, 3236. (m) Berger, R. M.; McMillin, D. R. *Ibid.* **1988**, *27*, 4245.

[4] (a) Braterman, P. S.; Heath, G. A.; Yellowlees, L. J. *J. Chem. Soc., Dalton Trans.* **1981**, 1801. (b) Kober, E. M.; Meyer, T. J. *Inorg. Chem.* **1982**, *21*, 3967. (c) *Ibid.* **1984**, *23*, 3877. (d) Braterman, P. S. *Ibid.* **1986**, *25*, 1732. (e) Yersin, H.; Gallhuber, E.; Hensler, G. *Chem. Phys. Lett.* **1987**, *134*, 497. (f) Ferguson, J.; Krausz, E. *Inorg. Chem.* **1987**, *26*, 1383. (g) Myrick, M. L.; Blakley, R. L.; DeArmond, M. K.; Arthur, M. L. *J. Am. Chem. Soc.* **1988**, *110*, 1325.

[5] (a) Krause, R. A. *Struct. Bonding Berlin* **1987**, *67*, 1. (b) Juris, A.; Balzani, V.; Barigelletti, F.; Campagna, S.; Belser, P.; von Zelewsky, A. *Coord. Chem. Rev.* **1988**, *84*, 85.

[6] Ernst, S. D.; Kaim, W. *Inorg. Chem.* **1989**, *28*, 1520.

[7] (a) Kaim, W. *Coord. Chem. Rev.* **1987**, *76*, 187. (b) von Zelewsky, A.; Daul, C.; Schläpfer, C. W. *Landolt-Börnstein, Physical and Chemical Tables*; Springer-Verlag: West Berlin, 1987; New Series, Vol. II/17a, p 199.

[8] (a) Rillema, D. P.; Allen, G.; Meyer, T. J.; Conrad, D. *Inorg. Chem.* **1983**, *22*, 1617. (b) Barigelletti, F.; Juris, A.; Balzani, V.; Belser, P.; von Zelewsky, A. *Ibid.* **1987**, *26*, 4115. (c) Tazuke, S.; Kitamura, N. *Pure Appl. Chem.* **1984**, *56*, 1269.

0002-7863/90/1512-173$02.50/0

$$[\mathrm{Ru^{II}(L)_3}]^{2+} \xrightarrow{e^-} [\mathrm{Ru^{II}(L)_2(L^{\bullet -})}]^{\bullet +} \qquad (1)$$

$$[\mathrm{Ru^{II}(L)_3}]^{2+} \xrightarrow[\mathrm{MLCT}]{h\nu} {}^*[\mathrm{Ru^{III}(L)_2(L^{\bullet -})}]^{2+} \qquad (2)$$

The MLCT excited state in such systems may be formulated as containing an anion-radical ligand (eq 2);[4,7] as in the reduced form (eq 1),[3] the question is[4] whether the unpaired (excited) electron is localized in the π^* orbital of only one chelate ligand (the concept of "spatially isolated redox orbitals")[3c] or whether delocalization and symmetrical spin distribution occur. An appreciable barrier for delocalization as illustrated by the electron hopping process (Scheme I)[3] is not unexpected since the π systems of the three unsaturated α-diimine ligands are not coplanar and thus only partially overlapping. Although the singly reduced species (eq 1) are just models for the MLCT excited state (eq 2) because they contain one more electron (d^6 vs d^5 metal configuration), a systematic attempt to understand this widely studied class[5] of complexes seems appropriate and should cover a large number of rather different ligand combinations.

Investigations of DeArmond, Hanck, and co-workes on 2,2′-bipyridine, 1,10-phenanthroline, and similar systems have indicated that the barrier for hopping in cationic complexes (eq 1) is such (500–1000 cm^{-1}) that it leads to broadening of ESR spectra;[3a-l] however, there are other additional factors contributing to unresolved ESR features for singly reduced tris(α-diimine)ruthenium complexes: Metal isotope coupling is expected to be small if the spin resides mainly on the ligand(s) (eq 1),[7a] especially since the pertinent nuclei ^{99}Ru and ^{101}Ru ($I = {}^5/_2$) have a rather small magnetic moment and relatively low combined natural abundance of 30%.[10] On the other hand, bpy anion-radical complexes are generally distinguished by a large number (405) of overlapping hyperfine lines from 2 N and 4 × 2 H nuclei, moreover, interaction of spin with, e.g., the ^{14}N nuclei[11] of nonreduced α-diimine ligands in a localized description (eq 1) via hyperconjugative spin transfer[7a,12] may further broaden ESR spectra through multiple overlap between hyperfine lines.

Localization in mono- or dinuclear polyazineruthenium radical complexes can be enforced by the introduction of strong asymmetry with one better acceptor ligand (L) and two other less π-accepting α-diimines such as bpy.[3e,10a,13] We have shown that such strategies can in some instances produce improved ESR resolution and the appearance of interpretable hyperfine structure for mono-[13] and dinuclear systems;[10a] similar results were reported later by Gex, DeArmond, Hanck, and co-workers.[3h-j] However, the peak-to-peak line widths ΔH_{pp} and the hyperfine structure are not the only parameters available from ESR studies; the g factor (the "chemical shift" of the radical) may be determined with considerable accuracy and can also provide insight into the frontier orbital situation[7a] as we have demonstrated for a number of anion-radical complexes.[10b,12b,d,14]

We now report ESR data (g, ΔH_{pp}, hyperfine features) of 16 singly reduced tris(α-diimine)ruthenium complexes (Chart I)[6] of which 6 are homoleptic (**1**–**6**), 5 are mononuclear bis(2,2′-bipyridine)ruthenium systems (**7**–**11**), and 5 are symmetrical dimers (**12**–**16**). Electrochemistry and spectroscopy of the precursor complexes have been described[2d,6,15] as have the calculated and experimental characteristics of the anion-radical ligands.[11,12b,14b,15,16]

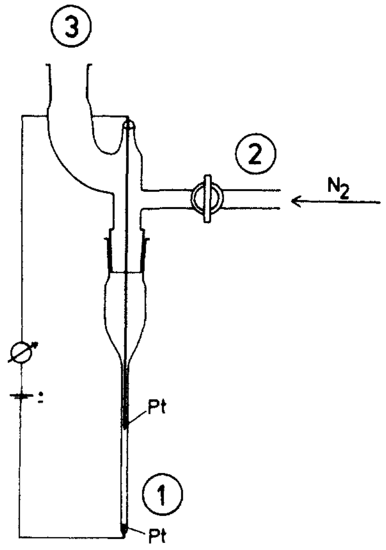

Figure 1. Electrolysis cell for intra muros ESR detection: platinum tip working electrode (1), nitrogen flushing valve (2), and port for introduction of substrate and electrolyte.

Chart I

$[\mathrm{Ru(bpy)_3}]^{\bullet +}$ (1)
$[\mathrm{Ru(bpdz)_3}]^{\bullet +}$ (2)
$[\mathrm{Ru(bpm)_3}]^{\bullet +}$ (3)
$[\mathrm{Ru(bpz)_3}]^{\bullet +}$ (4)
$[\mathrm{Ru(bpym)_3}]^{\bullet +}$ (5)
$[\mathrm{Ru(abpy)_3}]^{\bullet +}$ (6)
$[\mathrm{(bpy)_2Ru(bpdz)}]^{\bullet +}$ (7)
$[\mathrm{(bpy)_2Ru(bpm)}]^{\bullet +}$ (8)
$[\mathrm{(bpy)_2Ru(bpz)}]^{\bullet +}$ (9)
$[\mathrm{(bpy)_2Ru(bpym)}]^{\bullet +}$ (10)
$[\mathrm{(bpy)_2Ru(abpy)}]^{\bullet +}$ (11)
$[\mathrm{(bpy)_2Ru(\mu,\eta^4\text{-}bpym)Ru(bpy)_2}]^{\bullet 3+}$ (12)
$[\mathrm{(bpy)_2Ru(\mu,\eta^4\text{-}bppz)Ru(bpy)_2}]^{\bullet 3+}$ (13)
$[\mathrm{(bpy)_2Ru(\mu,\eta^4\text{-}bptz)Ru(bpy)_2}]^{\bullet 3+}$ (14)
$[\mathrm{(bpy)_2Ru(\mu,\eta^4\text{-}abpy)Ru(bpy)_2}]^{\bullet 3+}$ (15)
$[\mathrm{(bpy)_2Ru(\mu,\eta^4\text{-}bpip)Ru(bpy)_2}]^{\bullet 3+}$ (16)

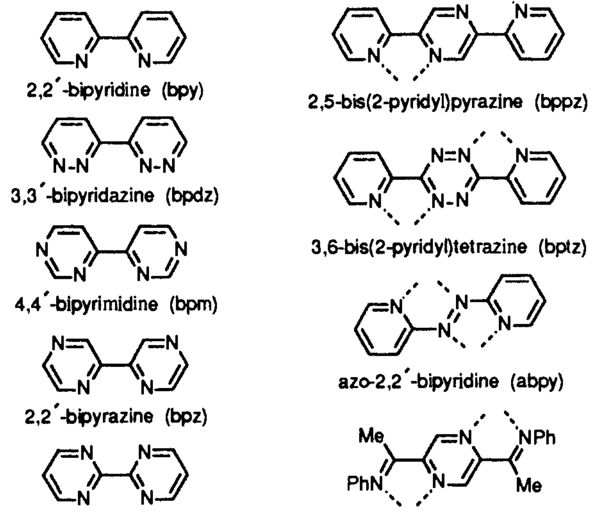

2,2′-bipyridine (bpy)
3,3′-bipyridazine (bpdz)
4,4′-bipyrimidine (bpm)
2,2′-bipyrazine (bpz)
2,2′-bipyrimidine (bpym)
2,5-bis(2-pyridyl)pyrazine (bppz)
3,6-bis(2-pyridyl)tetrazine (bptz)
azo-2,2′-bipyridine (abpy)
2,5-bis[1-(phenylimino)ethyl]pyrazine (bpip)

Experimental Section

Materials. The syntheses of the nonreduced precursor complexes of **1**–**15** have been described.[2d,6] The new bis-chelate ligand 2,5-bis[1-(phenylimino)ethyl]pyrazine (bpip) was obtained via condensation of 2,5-diacetylpyrazine[10b,17] with 2 equiv of aniline,[15] and the dinuclear complex **16** was synthesized from bpip and *cis*-Ru(bpy)$_2$Cl$_2$·2H$_2$O according to standard procedures.[2d,3h-j,6,10a]

---

(9) (a) Lehn, J. M.; Sauvage, J. P. *Nouv. J. Chim.* **1977**, *1*, 449. (b) Kalyanasundaram, K.; Kiwi, J.; Grätzel, M. *Helv. Chim. Acta* **1978**, *61*, 2720. (c) Prasad, D. R.; Hoffman, M. Z. *J. Am. Chem. Soc.* **1986**, *108*, 2568.

(10) (a) Kaim, W.; Ernst, S.; Kohlmann, S.; Welkerling, P. *Chem. Phys. Lett.* **1985**, *118*, 431. (b) Bessenbacher, C.; Ernst, S.; Kohlmann, S.; Kaim, W.; Kasack, V.; Roth, E.; Jordanov, J. *J. Chem. Soc., Faraday Trans. 1*, in press. (c) Kohlmann, S.; Kasack, V.; Roth, E.; Kaim, W. *Ibid.*, in press.

(11) Kaim, W. *Chem. Ber.* **1981**, *14*, 3789.

(12) (a) Kaim, W. *J. Organomet. Chem.* **1984**, *262*, 171. (b) Kaim, W. *Inorg. Chem.* **1984**, *23*, 3365. (c) Olbrich-Deussner, B.; Kaim, W. *J. Organomet. Chem.* **1988**, *339*, 253. (d) Ernst, S.; Kohlmann, S.; Kaim, W. *Ibid.* **1988**, *354*, 177.

(13) Ernst, S.; Kaim, W. *Angew. Chem.* **1985**, *97*, 431; *Angew. Chem., Int. Ed. Engl.* **1985**, *24*, 430.

(14) (a) Gross, R.; Kaim, W. *Inorg. Chem.* **1986**, *25*, 498. (b) Kaim, W.; Kohlmann, S. *Ibid.* **1986**, *25*, 3442. (c) Kaim, W.; Kohlmann, S. *Chem. Phys. Lett.* **1987**, *139*, 365.

(15) Kasack, V. Ph.D. Thesis, University of Stuttgart, West Germany, 1989.

(16) Kaim, W.; Ernst, S. *J. Phys. Chem.* **1986**, *90*, 5010.

(17) Caronna, T.; Fronza, G.; Minisci, F.; Porta, O. *J. Chem. Soc., Perkin Trans. 2* **1972**, 2035.

Scheme I

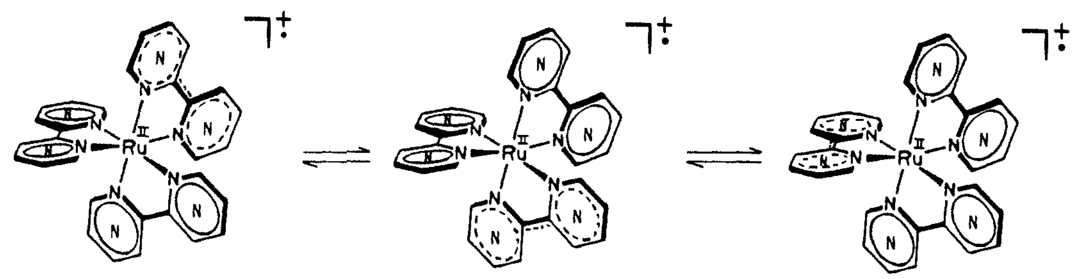

Table I. ESR Data of Mono- and Dinuclear Tris(α-diimine)ruthenium(II) Radical Complexes[a]

complex	compd no.	ΔH_{pp}[b]	g	$\Delta g\cdot 10^4$[c]	$E_{ox(1)}$[d]	$E_{ox(2)}$[d]	$\sum c_{N^2}$[h]
$\{Ru(bpy)_3\}^{\bullet +}$	**1**	5.0	1.9961	71	−1.31	1.27	0.278
$\{Ru(bpdz)_3\}^{\bullet +}$	**2**	1.8	1.9964	72	−1.00	1.58	0.326
$\{Ru(bpm)_3\}^{\bullet +}$	**3**	2.0	1.9982	51	−0.58	1.75	0.208
$\{Ru(bpz)_3\}^{\bullet +}$	**4**	2.0	1.9877	156	−0.68	1.98	0.340
$\{Ru(bpym)_3\}^{\bullet +}$	**5**	2.3	1.9983	47	−0.91	1.69	0.190
$\{Ru(abpy)_3\}^{\bullet +}$	**6**	3.1	1.9966	78	−0.02	>2.1	0.320
$\{Ru(bpy)_2(bpdz)\}^{\bullet +}$	**7**	1.8[f]	1.9908	128	−1.06	1.42	
$\{Ru(bpy)_2(bpm)\}^{\bullet +}$	**8**	1.0[e]	1.9973	60	−0.67	1.45	
$\{Ru(bpy)_2(bpz)\}^{\bullet +}$	**9**	1.1[e]	1.9910[g]	123	−0.91	1.49	
$\{Ru(bpy)_2(bpym)\}^{\bullet +}$	**10**	1.5[f]	1.9942	88	−1.02	1.40	
$\{Ru(bpy)_2(abpy)\}^{\bullet +}$	**11**	2.0[f]	1.9978	66	−0.36	1.60	
$\{[Ru(bpy)_2]_2(\mu\text{-bpym})\}^{\bullet 3+}$	**12**	1.4[e]	1.9890	140	−0.41	1.53	0.380
$\{[Ru(bpy)_2\}_2(\mu\text{-bppz})\}^{\bullet 3+}$	**13**	1.4	1.9896	140	−0.55	1.39	0.420
$\{[Ru(bpy)_2]_2(\mu\text{-bptz})\}^{\bullet 3+}$	**14**	2.0[e]	1.9980	60	−0.03	1.52	0.500
$\{[Ru(bpy)_2]_2(\mu\text{-abpy})\}^{\bullet 3+}$	**15**	2.0[f]	1.9984	60	+0.27	1.67	0.668
$\{[Ru(bpy)_2]_2(\mu\text{-bpip})\}^{\bullet 3+}$	**16**	1.5	1.9980[h]	64	−0.13	1.50	0.420

[a] From cathodic reduction of precursors in acetonitrile/0.1 M tetrabutylammonium perchlorate at 300 K. [b] Peak-to-peak line widths (mT) at low-modulation amplitude (<0.05 mT). [c] g(ligand anion radical) − g(Ru radical complex). [d] First two oxidation potentials (V vs SCE) of radical complexes (from ref 6). [e] Partially resolved spectrum (see text). [f] Structured spectrum. [g] $g = 1.9931$ in DME.[3h] [h] In acetone; $g_1 = 1.979$, $g_2 = 1.996$, $g_3 = 2.019$ in the partly reduced solid at 300 K. [i] Sum acetone; Hückel MO spin populations for coordinating nitrogen centers of anion-radical ligands (Coulomb integral parameters $h_N = 0.5$ for mononucleating and 0.8 for dinucleating chelate systems, from ref 20 and 25).

Instrumentation. ESR spectra were recorded on Varian E9, Varian 109, and Bruker ESP 300 spectrometers in the X-band. The modulation amplitude was kept below 0.05 mT in order to ensure the best resolution possible. Calibration and g factor determination (±0.0003) were done with the double-cavity technique with perylene anion radical[18] as the standard or by measurement of the magnetic field (Varian NMR gaussmeter) and microwave frequency (EIP 548A frequency counter).

Radical Generation. Singly reduced complexes **1**–**15** for ESR measurement were obtained by short intra muros electrolysis at the threshold potential[6] of dilute (10^{-4} M) solutions of precursor complexes in acetonitrile/0.1 M $Bu_4N^+ClO_4^-$ or by reduction with zinc dust in the same solvent (**14**). The two-electrode cell with a narrow i.d. = 1 mm is shown in Figure 1. The rather labile complex **16** was studied in acetone solution as was the system **14**[10a] at 3.7 K (glassy matrix).

ESR computer simulations were performed on XT or AT systems with available programs.[19]

Results

ESR spectra were obtained after cathodic reduction (eq 1) of precursors at ambient temperatures. In those cases where hyperfine features were observable, expanded spectra were computer simulated in order to analyze the hyperfine structure; one such spectrum is shown in Figure 2.

The best resolved ESR spectrum was observed for the complex $\{(\mu,\eta^4\text{-bptz}^{\bullet -})[Ru(bpy)_2]_2\}^{3+}$ and had been presented earlier.[10a] In order to further confirm the spin localization on the central

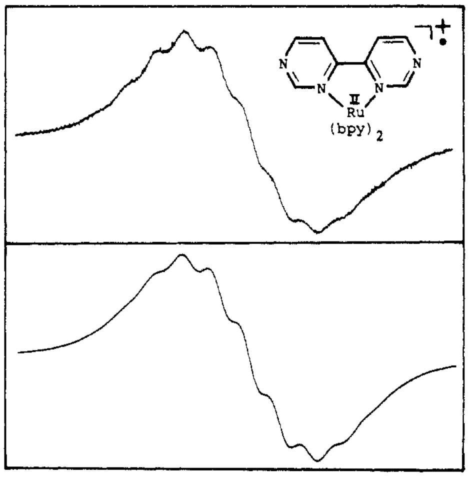

Figure 2. ESR spectrum of **8** in acetonitrile at 300 K (top) and computer simulation with the data reported in text (bottom).

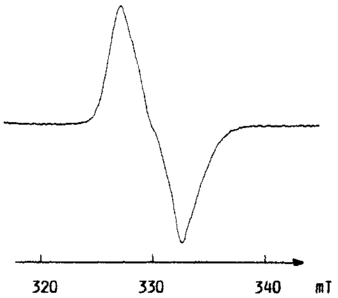

Figure 3. ESR spectrum of **14** at 3.9 K in frozen acetone solution (microwave frequency 9.2285 GHz). Hyperfine coupling[10a] and relatively small g anisotropy result in a little structured signal.

---

(18) Bolton, J. R. *J. Phys. Chem.* **1967**, *71*, 3702.

(19) (a) Oehler, U. M.; Janzen, E. G. *Can. J. Chem.* **1982**, *60*, 1542. (b) Isotope routine: Kaim, W.; Bock, H. *J. Organomet. Chem.* **1979**, *164*, 281. Cf. also: Schulz, A. Ph.D. Thesis, Universität Stuttgart, West Germany, 1989.

(20) Ernst, S.; Kaim, W. *J. Am. Chem. Soc.* **1986**, *108*, 3578.

(21) Kohlmann, S.; Ernst, S.; Kaim, W. *Angew. Chem.* **1985**, *97*, 698; *Angew. Chem., Int. Ed. Engl.* **1985**, *24*, 684.

(22) (a) Schneider, F.; Möbius, K.; Plato, M. *Angew. Chem. Int. Ed. Engl.* **1965**, *4*, 819. (b) Fischer, H. In *Free Radicals*; Kochi, J. K., Ed.; Wiley-Interscience: New York, 1973; Vol. II, p 452.

(23) Goodman, B. A.; Raynor, J. B. *Adv. Inorg. Chem. Radiochem.* **1970**, *13*, 135.

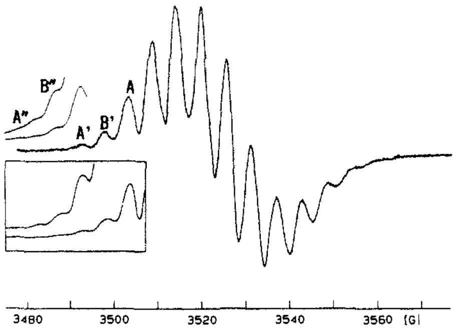

Figure 4. ESR spectrum of **14** at 300 K in acetonitrile with amplified low-field wing section. Computer simulation of that section (inset) reproduces the satellite lines due to isotope combinations with one (single prime) or two (double prime) ^{99,101}Ru isotopes ($I = {}^5/_2$, 29.8% natural abundance: $a_{^{99,101}\mathrm{Ru}}$ = 0.435 mT (2 Ru), $a_{^{14}\mathrm{N}}$ = 0.569 mT (4 N), 0.21-mT line width.

bridging bptz ligand, we now show the ESR signal as recorded in frozen acetone solution (Figure 3) and as recorded at high gain and high concentration after generation with zinc (Figure 4).

g factors, differences (Δg) between ligand anion radicals and the ruthenium radical complexes, peak-to-peak line widths ΔH_{pp}, oxidation potentials of the singly reduced complexes **1–16**, and the sums of Hückel MO-calculated[24] spin populations (c_{N^2}) at the coordinating centers of the anion-radical ligands[20,25] are summarized in Table I.

Discussion

(I) Line Widths and Hyperfine Structure. 1. Complexes $[\mathrm{Ru(bpy)_2(L^{\bullet-})}]^{\bullet+}$. All ligands used are better π acceptors than bpy.[6] The first electrochemical reduction wave of complexes $[\mathrm{Ru(bpy)_2(L)}]^{2+}$ is found at a distinctly more positive value than the following waves,[6] indicating the predominant localization of the first electron added on the most reducible ligand. ESR spectra of those systems, although sometimes totally unresolved, are yet distinctly narrower than those of corresponding homoleptic species (Figure 4) with their tendency to show additional line-broadening effects due to electron hopping (Scheme I).

The first reported[13] partially resolved spectrum is shown with its computer simulation in Figure 2. The coupling constants $a_{\mathrm{N}(1,1',3,3')}$ = 0.27 mT and $a_{\mathrm{H}(6,6')}$ = 0.23 mT for **8** are in agreement with HMO–McLachlan spin density calculations and with data from much better resolved metal carbonyl complexes of bpm$^{\bullet-}$;[16] this ligand has a much lower π^* level than bpy.[20] Accidental degeneracy of coupling constants of the chemically nonequivalent nitrogen centers and the assignment of the hydrogen coupling are compatible with the expected large perturbation[7a,10a,11] caused by a dicationic back-donating metal fragment within the ligand π system. The residual, fairly large line width can be attributed mainly to unresolved ^{1}H and ^{14}N (bpy) hyperfine splitting; a ruthenium isotope coupling from only one metal center cannot be conclusively extracted from ESR spectra of such limited resolution since decreasing resolution in the outer spectral regions is expected to occur because of anisotropic line broadening.[7a,12,14] Structured ESR spectra were also observed for the bpdz, bpz, bpym, and abpy complexes because of the relatively few major coupling constants of corresponding ligand anion radicals.[16] Our results confirm recent reports of a partially resolved spectrum of $[\mathrm{Ru(bpy)_2(bpz^{\bullet-})}]^+$ (**9**), the hyperfine splitting being in agreement with the calculted spin distribution and with ESR results for metal tetracarbonyl complexes.[16] On the other hand, the coupling extracted[3j] from the very poorly resolved spectrum of $[\mathrm{Ru(bpy)_2(bpym^{\bullet-})}]^+$ is incompatible with calculated spin distributions for bpym$^{\bullet-}$ or with the ESR data of its $\mathrm{Cr(CO)_4}$ complex.[12b]

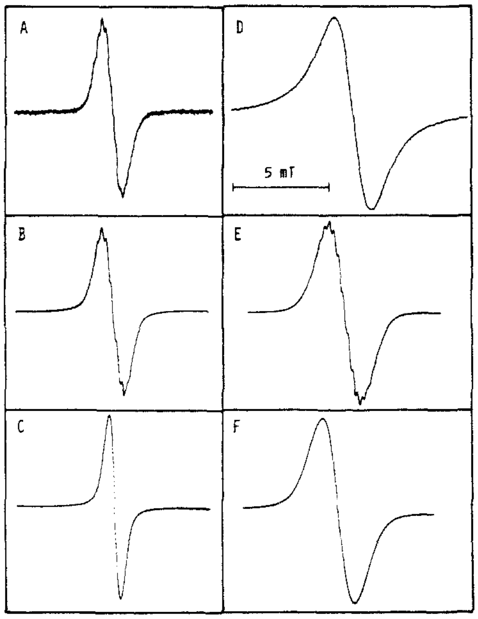

Figure 5. Experimental ESR spectra A (of **8**) and D (of **3**) and computer-generated spectra (B, C, E, F). For details, cf. text.

2. Complexes $[\mathrm{Ru(L)_3}]^{\bullet+}$. Attempts to determine the spin distribution in singly reduced tris(2,2′-bipyridine)ruthenium(II) have been inconclusive.[3a–f,l] The unusually broad ESR line of this particular species has been interpreted earlier as resulting from a dynamic exchange process (Scheme I) at the time scale of the ESR experiment;[3a] later attempts by the same group to use paramagnetic NMR techniques[3f] or high-temperature ESR in the oxidizing solvent DMSO[3l] did not unambiguously yield spin densities for individual centers because of lack of sufficient resolution.

We have previously reported that the three first reduction steps of the five other homoleptic complexes described here cover a range between 0.35 V (bpm) and 0.85 V (abpy system).[6] Despite separations between 0.15 V (bpm) and 0.35 V (abpy) for the first two reduction waves, there is no evidence for a structured, let alone resolved, ESR spectrum for the singly reduced homoleptic complexes **1–6** (Figure 5). All signals are distinctly broader than those obtained for the heteroleptic analogues. Figure 5 illustrates an attempt to assess the magnitude of broadening by computer simulations with use of Lorentzian line shape. Figure 5A,B shows the possible resolution as obtained and reproduced for the heteroleptic bpm system **8** (4 N, 0.27 mT; 2 H, 0.23 mT, 0.3 mT line width). In contrast, the experimental spectrum of $[\mathrm{Ru(bpm)_3}]^{\bullet+}$ (**3**) is unresolved and significantly broader (spectrum D). Computer simulations were first performed with the above set of coupling constants for 12 N and 6 H with 0.3 mT (Figure 5E) and 0.5 mT line width (spectrum F). However, a completely delocalized system may correspond rather to a simulation in Figure 5C (0.3 mT line width) where 12 N and 6 H were given one-third (N, 0.09 mT; H, 0.077 mT) of the coupling constants determined for the complex $[\mathrm{Ru(bpy)_2(bpm^{\bullet-})}]^+$ (Figure 5A,B). The experimental spectrum of $[\mathrm{Ru(bpm)_3}]^{\bullet+}$ is thus *always* broader than expected for a localized (Figure 5A,B) or completely delocalized situation (Figure C), in agreement with the notion of exchange broadening due to the process in Scheme I.[3a–e,h,j]

Within the series of the six homoleptic systems investigated, the broadness as measured by the peak-to-peak line width at low concentration and modulation amplitude is largest for the previously studied bpy system; the abpy complex and especially the bidiazine systems show this effect to a lesser extent. DeArmond and co-workers have calculated lower barriers to hopping (Scheme I) for the complexes **9**,[3h] **10**,[3j] and acceptor-substituted derivatives of **1**[3i] than for the bpy system; such a lower barrier is also assumed for other complexes with good π-accepting α-diimines and strongly facilitated reduction. However, this can only be an assumption

---

(24) (a) Gerson, F. *High Resolution E.S.R. Spectroscopy*; Wiley/Verlag Chemie: London/Weinheim, 1970. (b) Heilbronner, E.; Bock, H. *The HMO-Model and its Application*; Wiley/Verlag Chemie: London/Weinheim, 1976; p 308.

(25) Kaim, W.; Kohlmann, S. *Inorg. Chem.* **1987**, *26*, 68.

(26) Haga, M.; Dodsworth, E. S.; Lever, A. B. P. *Inorg. Chem.* **1986**, *25*, 447.

because the contributions from unresolved hyperfine splitting to the line width are different for each ligand system.[12b,16]

3. Complexes $\{[Ru(bpy)_2]_2(\mu\text{-}L^{\bullet-})\}^{\bullet 3+}$. Twofold coordination of $(bpy)_2Ru^{2+}$ electrophiles lowers the π^* level of a symmetrically bridging ligand more than single coordination.[6,21] Such reduced systems should therefore show an even more pronounced localization of spin on the "special" ligand than illustrated, e.g., in Figure 2; in fact, the first reduced ruthenium(II) polyazine complex with a sufficiently resolved ESR spectrum was the dimer **14**.[10a] Localization of spin within the bptz anion-radical ligand on the four nitrogen atoms in the central tetrazine ring[14b] has allowed determination of the approximate coupling constants $a_{^{14}N}$ as well as the $^{99,101}Ru$ isotope coupling.[10a] We were now able to observe and reproduce even the very weak lines from the combination with *two* spin-bearing isotopes, $^{99,101}Ru$, in the dinuclear complex (Figure 4), the probability of this combination being only 8.9%.[10a] The extracted parameters are in agreement with HMO–McLachlan perturbation calculations of the spin density and with a spin polarization mechanism for the metal isotope splitting.[10a,14b] Nevertheless, there is still a remaining line width of about 0.2 mT (Figure 4) that has to be attributed to unresolved coupling, e.g., from four axial bpy nitrogen atoms.

Other dinuclear systems with a more complicated hyperfine structure of the bridging anion-radical ligand gave less resolved ESR spectra; as in many other cases, care has to be exercised in interpreting spectra with poorly resolved ESR hyperfine structure. Such a spectrum of radical **12** was shown and interpreted with a rather large ruthenium coupling of 0.35 mT and a small H(5,5′) splitting of 0.137 mT;[3j] however, the ESR of **12** is perfectly reproduced by computer simulation employing the much more likely[10a,12b] values $a_{^{99,101}Ru}$ = 0.27 mT and $a_{H(5,5')}$ = 0.44 mT. The reported nitrogen coupling $a_{N(1,1',3,3')}$ = 0.274 mT[3j] is in agreement with our observations and with theory.[12b]

(II) *g* Factors and MO Spacing. *g* factors can be used to estimate the relative positions of frontier molecular orbitals,[22] especially if atoms with high spin–orbit coupling constants are participating. The general rule is[7a,12b,14a] that increasing participation of heavy atoms ($\xi(Ru) \approx 1000\ cm^{-1}$)[23] causes a stronger deviation of *g* from the value g_e = 2.0023 of the free electron, while the relative distance between the SOMO and the corresponding lowest totally unoccupied MO on one hand and the SOMO and the relevant doubly occupied MO on the other hand determine the *sign* of that deviation. See eq 3, where E_0 = energy of singly occupied molecular orbital, E_n = energies of empty or doubly occupied MOs, ξ_k = spin–orbit coupling constant, and **L** = angular momentum operator[22b]

$$g = g_e - {}^2\!/_3 \sum_i \sum_n \sum_{k,j} \frac{\langle \psi_0 | \xi_k \mathbf{L}_{ik} \delta_k | \psi_n \rangle \langle \psi_n | \mathbf{L}_{ij} \delta_j | \psi_0 \rangle}{E_n - E_0} \qquad (3)$$

Table I summarizes the observed isotropic *g* factors of the singly reduced ruthenium monomers and dimers together with the deviation Δg from the values of the free-ligand anion radicals. This quantity is more significant than the difference between *g*(complex) and g_e because the large and generally variable spin densities at the nitrogen atoms[14b,16] also affect the deviation $g - g_e$. We have to neglect, therefore, the coordination induced changes in the overall spin distribution caused by metal coordination.

1. Homoleptic Complexes. When the isotropic *g* values of the singly reduced four isomeric bidiazine systems, the $(bpy)_3$ and $(abpy)_3$ complexes (Table I) are compared, two factors have to be considered:

(i) The contribution from the heavy-metal center is largest for those complexes that allow the most effective spin transfer via the coordinating nitrogen centers (the "metal–ligand interface"[6]). This effect has been demonstrated in a number of cases where calculated HMO spin populations (= squared Hückel molecular orbital coefficients c_{N^2}; Table I)[24] were successfully correlated to metal fragment coupling constants.[12c,d,14b,c,16] A survey of the Δg values in Table I shows indeed that complexes of those ligands with large overall chelate N spin populations (bpz, bpdz, abpy)[14b,16] exhibit larger deviations than the other cation radicals with bpy, bpm, or bpym ligands.

Chart II

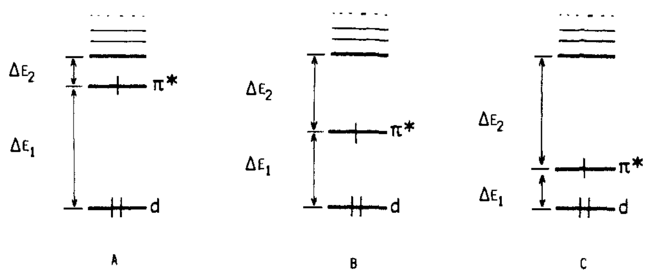

(ii) the *sign* of Δg is, to a first approximation, determined by the relation between the two energy differences ΔE_1 and ΔE_2 (eq3, Chart II). This relation may be estimated from redox potential differences, transition energies, or MO calculations; three identical chelate ligands give rise to two close-lying π^* orbitals (e, a_2) in D_3 symmetry.[4b,c] On the other hand, stabilization of occupied d levels should result in a large ΔE_1 and thus lead to increased deviation of *g*(ligand) from *g*(complex). In fact, the complexes where the (metal-centered) second oxidation $E_{ox(2)}$ of the radical species occurs at the most positive potentials (abpy, bpz)[6] show the largest deviations Δg. The particularly strong effect for the bpz derivative **4** is connected to a small ΔE_2 as indicated by only 0.19- and 0.27-V difference between the first three reduction waves,[6] whereas the abpy system shows much larger potential differences (0.35 and 0.50 V).[6]

2. Heteroleptic Complexes. The result that *all* complexes $[(\alpha\text{-diimine}^{\bullet-})Ru(bpy)_2]^+$ have isotropic *g* factors smaller than g_e and even smaller than 2 may be interpreted[10a] as a consequence of the additional low-lying π^* orbitals of the bpy coligands, creating a situation such as A in Chart II with rather small energy differences between π^*(α-diimine) and π^*(bpy) orbitals. The latter may serve as an internal reference[27b] and thus allow an estimation of the relation $\Delta E_1/\Delta E_2$. Low-lying, ligand field excited states[4b,c] may also contribute to the decrease of *g*(complex),[12d,14a] and the changes in *g* are influenced again by the two factors (i and ii) mentioned above. This time, however, the ΔE_2 increases clearly with the increasing π-acceptor capability[20,25] of the special α-diimine ligand so that the bpdz system with large $c_N{}^2$ and a π^*(bpdz) level close to that of π^*(bpy)[20] exhibits the largest deviation Δg whereas the reduced bpm complex with small $c_N{}^2$ values and a stabilized LUMO[20] shows the smallest difference. In case of the other mononuclear $(bpy)_2Ru^{II}$ radical complexes effects i and ii compensate to varying extents, the Δg showing intermediate values.

The dinuclear complexes fall into two categories: Systems with not too stabilized SOMO levels (bpym, bppz, intermediate ΔE_2) show primarily the effect of double-metal participation via an approximate doubling of the Δg shift (bpym example). On the other hand, those ligands (bptz, abpy, bpip) with very low-lying π^* orbitals[25] exhibit a relatively small lowering of *g* because these ligand orbitals and the π^*(bpy) levels are now quite far apart ($\Delta E_2 \approx \Delta E_1$, situation B in Chart II). A reversal of the sign of Δg has been observed for $(bpy)_2Ru^{II}$ complexes of oxygen-containing anion radicals such as semiquinones with still lower lying π^* orbitals.[26,27] In those instances, ΔE_1 can become considerably smaller than ΔE_2 (situation C in Chart II),[27b] while strong d/π^* mixing may lead to large absolute values of Δg due to contributions (eq 3) from the heavy-metal centers.[28]

3. *g* Anisotropy. ESR spectra of the singly reduced complexes in frozen solution or of partially reduced solid materials exhibit little anisotropy (Figure 3) as has already been discussed for other species related to $(bpy)_3Ru^{\bullet+}$.[3] The dinuclear complexes **14** (Figure 3) and **15** (Table I) show a somewhat stronger effect

---

(27) (a) Ernst, S.; Hänel, P.; Jordanov, J.; Kaim, W.; Kasack, V.; Roth, E. *J. Am. Chem. Soc.* **1989**, *111*, 1733. (b) Ernst, S.; Kasack, V.; Bessenbacher, C.; Kaim, W. *Z. Naturforsch. B: Anorg. Chem. Org. Chem.* **1987**, *42b*, 425.

(28) Kaim, W.; Kasack, V.; Binder, H.; Roth, E.; Jordanov, J. *Angew. Chem.* **1988**, *100*, 1229; *Angew. Chem., Int. Ed. Engl.* **1988**, *27*, 1174.

because of 2-fold ruthenium participation; however, even these data are clearly compatible[7a] with an overwhelming ligand character of the singly occupied MO. Major anisotropy effects appear, however, if carbonyl-containing radical ligands with strong mixing of ligand and metal orbitals are employed.[26-28]

The results from this ESR study support the interpretation of spectroscopic and electrochemical differences between the redox series involving compounds **1**–**16**.[6] Furthermore, the results support the hopping model[3a-f] for homoleptic tris(ligand) systems on the time scale of the ESR experiment and show the effects of localization for heteroleptic systems. In spite of the limited information available from poorly resolved ESR spectra with very little *g* anisotropy, even the isotropic *g* factors of the radical complexes have proven valuable for analysis of the electronic structure: As has been demonstrated in previous studies,[12,14] the presence of more than one low-lying unoccupied orbital in nonreduced precursor complexes (and corresponding photoreactivity)[12,14] may be correlated via Chart II to small *g* values of the singly reduced complexes.

Acknowledgment. This work has been generously supported by Deutsche Forschungsgemeinschaft and Stiftung Volkswagenwerk. We also thank Degussa AG for a donation of chemicals and Dipl.-Chem. E. Roth and Dr. J. Jordanov (CENG, Grenoble, France) for assistance with the low-temperature ESR measurements.

Mechanisms of Reactions of Iron(III) Porphyrins with Hydrogen Peroxide and Hydroperoxides: Solvent and Solvent Isotope Effects

Teddy G. Traylor* and Feng Xu

Contribution from the Department of Chemistry, D-006, University of California, San Diego, La Jolla, California 92093. *Received March 22, 1989*

Abstract: The effect of solvent polarity and acidity and the solvent isotope effects on the reaction of iron(III) porphyrins with hydrogen peroxide, *tert*-butyl hydroperoxide, and peracids have been investigated. Both the solvent and solvent isotope effects on the reactions of hydroperoxides with hemins are almost identical with these effects on the reactions of hydroperoxides with dialkyl sulfides and the effects on the reaction of peracids with iron(III) porphyrins. Since both of the latter reactions are known to involve heterolytic cleavage of the O–O bond, this similarity provides strong evidence for heterolytic cleavage of hydroperoxide by reaction with hemins. The strong alcohol catalysis of the studied reactions provides a mechanistic rationale for the O–O bond cleavage in cytochrome P-450 in terms of general-acid catalysis by water in the enzyme site.

The reactions of hydrogen peroxide with peroxidases and catalase result in heterolytic cleavage of the oxygen–oxygen bond to produce a two-electron-oxidized "oxene" species,[1,2] also recently identified by using model hemin compounds.[3] Crystal structures of cytochrome *c* peroxidase[4] and catalase[5] reveal a general-acid/general-base apparatus in proper juxtaposition to assist the hydroxide leaving group, proposed to occur as shown.

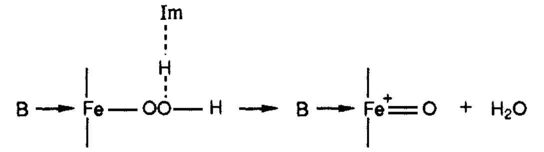

(1)

This general-acid/general-base process has been mimicked in model systems with the demonstration that cleavage of peracids and hydroperoxides by simple hemins is catalyzed by added buffers[6-8] and by covalently attached bases or carboxylic acids[6a] as well as by electron donation by hemin substituents[6a] and by hydrogen bonding to the proximal imidazole.[6c,7c] Mechanisms for the general-base- and general-acid-catalyzed processes have therefore been concluded to occur as follows.[6-8]

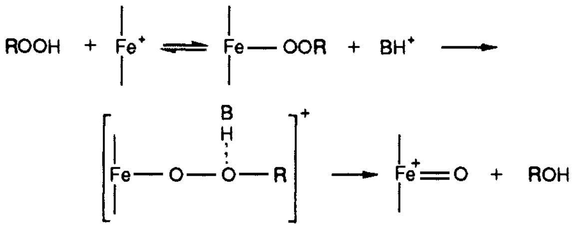

(2)

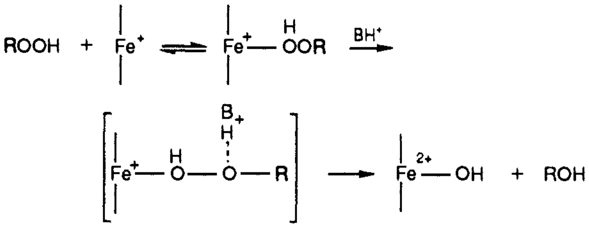

(3)

A simplified form of the transition state in eq 2 is often written[6,7] as

---

(1) (a) Dunford, H. B.; Stillman, J. S. *Coord. Chem. Rev.* **1976**, *19*, 187. (b) Hewson, W. D.; Hager, L. P. In *The Porphyrins*; Dolphin, D., Ed.; Academic: New York, 1979; Vol. VII.

(2) (a) Deisseroth, A.; Douce, A. L. *Physiol. Rev.* **1970**, *50*, 319. (b) Schonbaum, G. R.; Chance, B. In *The Enzymes* (3rd Ed.); Boyer, P. D., Ed.; Academic: New York, 1976; Vol. 13, p 363.

(3) Groves, J. T.; Haushalter, R. C.; Nakamura, M.; Nemo, T. E.; Evans, B. J. *J. Am. Chem. Soc.* **1981**, *103*, 2884.

(4) (a) Poulos, T. L.; Freer, S. T.; Alden, R. A.; Edwards, S. L.; Skogland, U.; Takio, K.; Eriksson, B.; Xuong, N.; Yonetani, T.; Kraut, J. *J. Biol. Chem.* **1980**, *255*, 575. (b) Poulos, T. L.; Kraut, J. *Ibid.* **1980**, *255*, 8199.

(5) Vainshtein, B. K.; Melik-Adamyan, W. R.; Barynin, V. V.; Vagin, A. A.; Grebenko, A. I.; Borisov, V. U.; Bartels, K. S.; Fita, I.; Rossmann, M. G. *J. Mol. Biol.* **1986**, *88*, 49.

(6) (a) Traylor, T. G.; Lee, W. A.; Stynes, D. V. *J. Am. Chem. Soc.* **1984**, *106*, 755. (b) Traylor, T. G.; Popovitz-Biro, R. *Ibid.* **1988**, *110*, 239. (c) Traylor, T. G.; Ciccone, J. P. *J. Am. Chem. Soc.*, in press. (d) Ciccone, J. P.; Fann, W. P.; Xu, F., unpublished.

(7) (a) Zipplies, M. F.; Lee, W. A.; Bruice, T. C. *J. Am. Chem. Soc.* **1986**, *108*, 4433. (b) Bruice, T. C.; Zipplies, M. F.; Lee, W. A. *Proc. Natl. Acad. Sci. U.S.A.* **1986**, *83*, 4646. (c) Lee, W. A.; Yuan, L. C.; Bruice, T. C. *J. Am. Chem. Soc.* **1988**, *110*, 4277. (d) Balasubramanian, P. N.; Schmidt, E. S.; Bruice, T. C. *Ibid.* **1987**, *109*, 7865. (e) Zipplies, M. F.; Lee, W. A.; Bruice, T. C. *Ibid.* **1986**, *108*, 4443. (f) Bruice, T. C.; Balasubramanian, P. N.; Lee, R. W.; Lindsay Smith, J. R. *Ibid.* **1988**, *110*, 7891. (g) Lindsay Smith, J. R.; Balasubramanian, P. N.; Bruice, T. C. *Ibid.* **1988**, *110*, 7411.

(8) Groves, J. T.; Watanabe, Y. *J. Am. Chem. Soc.* **1986**, *108*, 507, 7834.

0002-7863/90/1512-178$02.50/0